

Multiaxial deformations of end-linked poly(dimethylsiloxane) networks.

4. Further assessment of the slip-link model for chain-entanglement effect on rubber elasticity

Kenji Urayama^{a)}

Institute for Chemical Research, Kyoto University, Uji, Kyoto-fu 611-0011, Japan

Takanobu Kawamura

Faculty of Materials and Design, Kyoto Institute of Technology, Matsugasaki, Sakyo-ku, Kyoto 606-8585, Japan

Shinzo Kohjiya

Institute for Chemical Research, Kyoto University, Uji, Kyoto-fu 611-0011, Japan

(Received 30 October 2002; accepted 3 January 2003)

The Edwards–Vilgis slip-link model for the chain-entanglement effect on rubber elasticity is critically assessed on the basis of quasiequilibrium biaxial stress–strain data of end-linked polydimethylsiloxane (PDMS) networks with different entanglement densities. The PDMS networks with different entanglement densities were prepared by end-linking end-reactive long precursor PDMS in solutions with different solvent contents. The slip-link model, in which trapped entanglement is modeled by fictitious mobile slip-link attaching two entangled chains, satisfactorily describes the biaxial data over the entire range of deformation for all the networks examined. The model-specific parameters, i.e., slippage of slip-link (η) and inextensibility of network (α), were employed as adjustable parameters in data-fitting. The fitted values of η and α vary reasonably with the degree of dilution at network preparation, i.e., entanglement density. With an increase in dilution, i.e., decrease in entanglement density, η increases, whereas α decreases. In addition, the fitted values of η and α are in good agreement with the estimates from another molecular approach independent of mechanical testings: $\eta = M_e/M_c$, where M_e and M_c are the molecular masses between neighboring entanglements and between adjacent cross-links, respectively; $\alpha = n_j^{-1/2}$, where n_j is the number of Kuhn segments between adjacent elastically effective junctions including cross-links and trapped entanglements. The satisfactory data-fit with the model parameters of physically reasonable magnitudes supports the validity of the slip-link model for entanglement effects on rubber elasticity. © 2003 American Institute of Physics. [DOI: 10.1063/1.1555636]

I. INTRODUCTION

High elasticity of cross-linked rubbers is dominantly entropic in origin, so that the main aim of molecular theory is to consider how the number of configurations available to the constituent polymers changes under deformation. On the basis of entropic elasticity of a single Gaussian chain, the classical rubber elasticity theories derived the elastic free energy (F) for a network composed of “phantom chains” which may pass freely through its neighbors,^{1–5}

$$\frac{F}{RT} = \frac{1}{2} C \left(\sum_{i=1}^3 \lambda_i^2 - 3 \right), \quad (1)$$

where R is the gas constant, T is the absolute temperature, λ_i ($i=1,2,3$) is the principal ratio in the i th coordinate direction, and C is a constant related to network structure such as the numbers of elastic chain and cross-link. The system comprised of phantom chains is essentially like an ideal gas with-

out any intermolecular interactions, and the Gaussian chain model yields an infinite extensibility of networks. Meanwhile, the real rubbery network has many chain-entanglements due to uncrossability of the network chains as well as a finite extensibility resulting from the full stretching of the network chains. Most of the entanglements in cross-linked polymers are permanently trapped due to the presence of cross-links, so that the trapped entanglements provide topological constraints yielding additional elastic free energy. The finite extensibility effect, which is often recognizable as an appreciable upturn of stress at high elongation in the uniaxial stress–strain curve, is not described by Eq. (1).

Modeling of entanglement effects has been a main focus of modern molecular theories of rubber elasticity, and several different entanglement models have been proposed. Recently, we have experimentally tested five molecular models which employ different treatments of entanglement effects (diffused-constraint model,⁶ slip-link model,⁷ the tube models of several versions^{8–10}) on the basis of quasiequilibrium “general biaxial” stress–strain data for an entanglement-dominated network of end-linked poly(dimethylsiloxane) (PDMS).¹¹ Some of the models^{7,9} also consider the non-Gaussian (finite extensibility) effect. General biaxial defor-

^{a)}Author to whom correspondence should be addressed. Present address: Faculty of Engineering, Department of Material Chemistry, Kyoto University, Sakyo-ku, Kyoto 606-8501, Japan. Electronic mail: urayama@rheogate.polym.kyoto-u.ac.jp

mation varying independently each of two principal strains (general biaxial strains) is one of the most rigorous experimental assessments to identify the models which account for the entanglement effect most successfully and correctly, because general biaxial strains achieve the whole accessible pure homogeneous deformations for an incompressible material.^{5,12} The arguments relying on only simple uniaxial deformation are insufficient to distinguish unambiguously the difference between the models, because uniaxial deformation is only a particular one among all the accessible deformations. Among the five theoretical models tested,¹¹ the predictive capability of the slip-link model was obviously superior to those of the other models, and the slip-link model satisfactorily described the biaxial data using the fitted parameters with the physically reasonable magnitudes.

To assess further strictly a molecular entanglement theory, it is very important to survey the predictive capability for the biaxial data of rubbery networks with different entanglement densities. Brereton *et al.*¹³ analyzed the uniaxial elongation data of cross-linked polyethylenes with different cross-linking density on the basis of the slip-link model, but their samples had a nonhomogeneous network structure due to cross-linking in the semicrystalline phase. The complicated structure of the samples as well as the analysis using only the uniaxial data made their assessment ambiguous. An appropriate way to control the entanglement density in the network is to end-link the precursor polymers in solution and vary the polymer concentration. Entanglement density in the end-linked network is significantly influenced by an overlapping degree of precursor chains before end-linking.¹⁴⁻¹⁸ In addition, the end-linking system enables us to estimate the parameters of the network structure such as the number of network chains and cross-links independently of mechanical testing, on the basis of a nonlinear polymerization theory¹⁹ with the data of the soluble fractions. This is advantageous relative to conventional randomly-crosslinked systems whose structural parameters are obscure.

In the present study, we assess further rigorously the slip-link model on the basis of the biaxial data of the end-linked PDMS networks with four different entanglement densities which are prepared from the melt and the solutions with three different precursor concentrations. In addition, we investigate how each of the best-fit model parameters depends on the degree of dilution at network preparation, i.e., entanglement density. The biaxial data of these four PDMS networks were originally employed in our separate study,²⁰ where the form of F was phenomenologically estimated using the two invariants of the deformation tensor as independent variables.²¹ This approach is entirely phenomenological, and the main objective is drastically different from that in the present study.

II. THE SLIP-LINK MODEL

The elastic free energy of the slip-link model consists of the two contributions originating from chemical cross-links and trapped entanglements.⁷ The expression of the former contribution due to chain connectivity is based on the Gaussian form which was derived by the classical rubber elasticity theory. The latter contribution due to trapped entanglements

are modeled by a number N_s of fictitious mobile slip-links which attach two entangled chains. The measure of slippage of slip-link, compared to that of a cross-link, is given by a parameter η . In the lower limiting case where the slippage becomes zero ($\eta=0$), the slip-link acts in the same way as the cross-link and fully contributes to the network modulus. In the upper limiting case where the slippage becomes infinitely large ($\eta=\infty$), the constraints by entanglements are extremely weak and the slip-link does not contribute to the network elasticity.

Edwards and Vilgis⁷ introduced the effect of finite network extensibility to the original slip-link model²² on the basis of the primitive path concept. The chain between entanglements is fully stretched long before the single chain between cross-links is taut when the network is deformed. As a result, the network extensibility is much lower than the extensibility of a single network chain between cross-links. The Edwards-Vilgis slip-link model has the singularity in the chain entropy at the ultimate elongation ratio λ_{\max} which is given by $\lambda_{\max}=n_j^{1/2}$, where n_j is the number of the Kuhn segments between adjacent elastically effective junctions. The limited network extensibility effect is introduced by the parameter α which is equal to λ_{\max}^{-1} . The full expression of the free energy of the Edwards-Vilgis slip-link model is given by

$$\begin{aligned} \frac{F}{RT} = & \frac{1}{2} N_c \left[\frac{(1-\alpha^2)\sum \lambda_i^2}{1-\alpha^2\sum \lambda_i^2} + \ln\left(1-\alpha^2\sum \lambda_i^2\right) \right] \\ & + \frac{1}{2} N_s \left[\sum \left\{ \frac{\lambda_i^2(1+\eta)(1-\alpha^2)}{(1+\eta\lambda_i^2)(1-\alpha^2\sum \lambda_i^2)} \right. \right. \\ & \left. \left. + \ln(1+\eta\lambda_i^2) \right\} + \ln\left(1-\alpha^2\sum \lambda_i^2\right) \right], \end{aligned} \quad (2)$$

where Σ denotes the summation for i from 1 to 3, and λ_i is the principal ratio in the i th direction. The elastic contribution of network connectivity, N_c , is related to the number densities of the network chain (ν) and cross-link (μ),²³

$$N_c = (\nu - h\mu), \quad (3)$$

where h is an empirical parameter varying from zero (affine limit) to unity (phantom limit) which depends on the degree of thermal fluctuation of the cross-link. In the case of $\alpha=0$ (i.e., infinite extensibility), Eq. (2) coincides with the free energy of the original slip-link model. Furthermore, $\eta=\alpha=0$ yields the classical free energy expressed by Eq. (1).

Theoretical stress-strain relation for a network biaxially stretched in the 1- and 2-directions ($\sigma_3=0$) is obtained using the following Treloar relations:⁵

$$\sigma_i = \frac{2}{V\lambda_i} \left[\lambda_i^2 \left(\frac{\partial F}{\partial \lambda_i^2} \right) - \lambda_3^2 \left(\frac{\partial F}{\partial \lambda_3^2} \right) \right]_{T,\nu} \quad (i=1,2), \quad (4)$$

where V is the volume of the network, and σ_i is the nominal stress (the force per unit area of undeformed state) in the i th direction. The principal ratio λ_3 is automatically determined by the relation $\lambda_3=(\lambda_1 \lambda_2)^{-1}$ due to incompressibility of the rubbery network. The expression of $\partial F/\partial \lambda_i^2$ is given by

TABLE I. Characteristics of end-linked PDMS networks.

Initial conc. /wt. %	$w_{\text{sol}}^{\text{a}}/\text{wt. \%}$	ϕ_0	r	$G_0^{\text{b}}/\text{kPa}$	$\nu^{\text{c}}/\text{mol m}^{-3}$	$\mu^{\text{c}}/\text{mol m}^{-3}$	$M_{n,\text{el}}^{\text{c}}/\text{kg mol}^{-1}$
100	8.76	0.914	1.3	144	5.88	3.71	77.4
70	7.50	0.625	1.3	64.9	3.22	2.04	82.5
50	3.69	0.463	1.3	24.5	3.02	1.90	73.8
30	1.66	0.283	1.3	8.69	2.12	1.32	69.3

^aFor reactants excluding unreactive diluent (initial conc.) + $w_c = w_{\text{sol}} + \rho_{\text{PDMS}}\phi_0$ where w_c and ρ_{PDMS} are the weight fraction of cross-linker and the density of PDMS, respectively.

^bFrom biaxial elongation experiment (Refs. 20, 21).

^cFrom the Miller–Macosko model (Ref. 19) for nonlinear polymerization.

$$\begin{aligned} \frac{\partial F}{\partial \lambda_i^2} = & \frac{1}{2} N_c RT \frac{(1 - 2\alpha^2 + \alpha^4 \sum \lambda_i^2)}{A^2} \\ & + \frac{1}{2} N_s RT \left(\frac{(1 + \eta)(1 - \alpha^2)}{A(1 + \eta \lambda_i^2)^2} + \frac{\eta}{1 + \eta \lambda_i^2} - \frac{\alpha^2}{A} \right. \\ & \left. + \sum \frac{(1 + \eta)(1 - \alpha^2)\alpha^2 \lambda_i^2}{A^2(1 + \eta \lambda_i^2)} \right), \end{aligned} \quad (5)$$

where $A = 1 - \alpha^2 \sum \lambda_i^2$.

Equilibrium (small-strain) shear modulus G_o of the slip-link model consists of the two contributions each of which originates from chemical connectivity and trapped entanglements,

$$\begin{aligned} \frac{G_o}{RT} = & N_c \frac{1 - 2\alpha^2 + O(\alpha^4)}{(1 - 3\alpha^2)^2} \\ & + N_s \frac{1 - 2\alpha^2 + 2\alpha^2 \eta + 2\alpha^2 \eta^2 + O(\alpha^4)}{(1 + \eta)^2 (1 - 3\alpha^2)^2}. \end{aligned} \quad (6)$$

Equation (6) is of the Greasley–Langley form^{23,24} where entanglement is treated as the localized additional cross-link contributing to the modulus.

III. CHARACTERISTICS OF THE END-LINKED PDMS NETWORKS

A. Uni- and biaxial elongation

The quasiequilibrium stress–strain data of uniaxial and biaxial deformations were obtained at 40 °C. The quasiequilibrium stress where the time effect was sufficiently eliminated was measured at each strain by the stress relaxation method. The details of the methods and instruments are described elsewhere.^{20,21}

B. Structural parameters

The end-reactive linear precursor PDMS used is long enough to form entanglement couplings before end-linking: The number-average molecular mass of the precursor ($M_{n,p} = 4.66 \times 10^4$ g/mol) is much larger than the critical molecular mass to form entanglement couplings for PDMS ($M = 1.66 \times 10^4$ g/mol).²⁵ The molar ratio of functional groups in the precursor to those in the tetrafunctional silane (cross-linker) (r) was 1.3 for all the samples. Oligodimethylsiloxane with $M = 3000$ was employed as a nonvolatile diluent. Four end-linked PDMS networks with different en-

tanglement densities were prepared from melt and the solutions of the precursor concentrations 70, 50, and 30 wt. %, respectively. The details of the sample preparation are referred to in our previous paper.²⁰ After the end-linking reaction, the resulting networks were used for mechanical measurements without removing the diluent. The weight fraction of the unreacted reactants (w_{sol}) was evaluated by extraction in toluene. Volume fraction of the precursor chain incorporated into the network (ϕ_0) was calculated by subtracting w_{sol} from the initial precursor concentration.

The molecular parameters characterizing the network structure, i.e., number densities of elastic network chains (ν) and cross-links (μ), the number-average molecular mass of elastic chains between cross-links (excluding any attached dangling chains) ($M_{n,\text{el}}$), were estimated using a nonlinear polymerization model for end-linking¹⁹ with the w_{sol} data. The estimated values of these parameters for each sample are summarized in Table I.

As can be seen in Table I, the $M_{n,\text{el}}$ values for the different networks are comparable, which indicates that the degree of dilution at network preparation alters the entanglement density of the resulting network without increasing significantly the network defects such as dangling chains and inelastic loops: If the degree of dilution increases the network defects, the resulting $M_{n,\text{el}}$ values will not be constant against ϕ_0 . The larger values of $M_{n,\text{el}}$ relative to $M_{n,p}$ is due to the nonstoichiometric ratio ($r \neq 1$) as well as the finite values of w_{sol} . Thus a main difference in network structure between the networks with different ϕ_0 is that of entanglement density.

IV. RESULTS AND DISCUSSIONS

Four parameters, h , N_s , η , α , are employed as adjustable parameters in the data-fitting procedure. The best-fit condition was determined so that the error Δ would be minimum,

$$\Delta = \frac{1}{2n} \left\{ \sum_{i=1,2} \sum_{m=1}^n \left(\frac{\sigma_{i,\text{exp}}^m - \sigma_{i,\text{th}}^m}{\sigma_{i,\text{exp}}^m} \right)^2 \right\}^{1/2}, \quad (7)$$

where n is the number of experimental data points, σ_{exp} and σ_{th} are experimental and theoretical stresses, respectively.²⁶ The fitting procedure yields a unique parameter set which can reproduce the most successfully the experimental data. In the minimization of Δ , each parameter was independently varied in the physically admissible range. For N_s without the upper limit, the theoretical value of G_0 was used as a cutoff

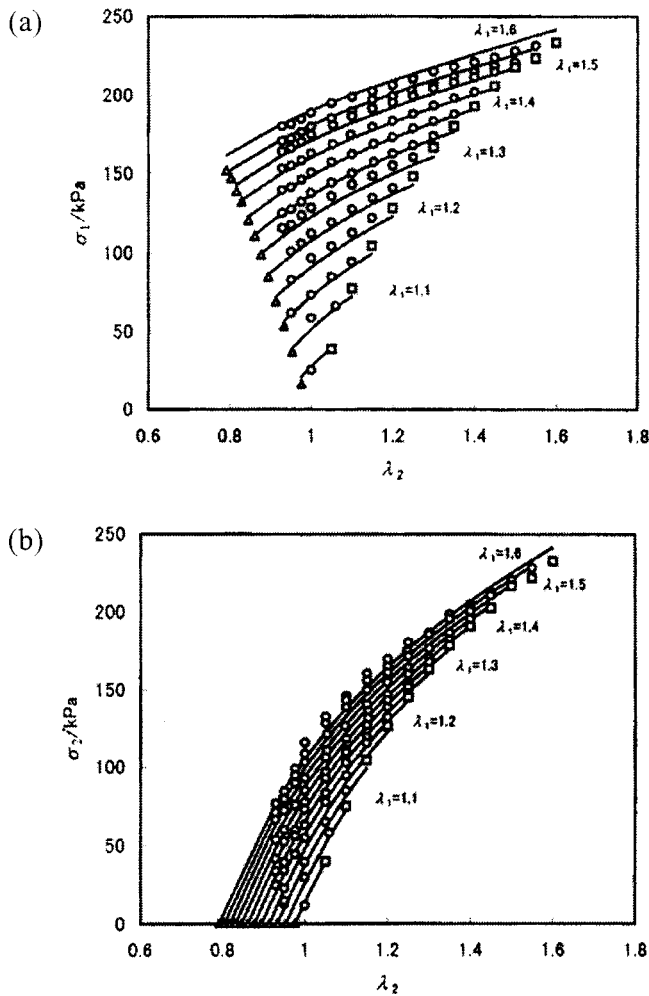


FIG. 1. Comparison of the theory with the quasiequilibrium biaxial stress–elongation data (Ref. 21) of the end-linked PDMS network of $\phi_0=0.914$. λ_1 and λ_2 are the larger and smaller principal ratios in biaxial stretching, respectively, and σ_1 (a) and σ_2 (b) are the nominal stresses in the corresponding directions. The triangular and rectangular symbols stand for the data for the uniaxial ($\lambda_2=\lambda_1^{-1/2}$ and $\sigma_2=0$) and equibiaxial stretching ($\lambda_1=\lambda_2$), respectively. The solid lines represent the theoretical stress σ_i ($i=1,2$) at identical λ_1 as a function of λ_2 . The best-fitted parameters are $N_s/N_c=8.98$, $\eta=0.105$, $\alpha=0.178$, $h=0$.

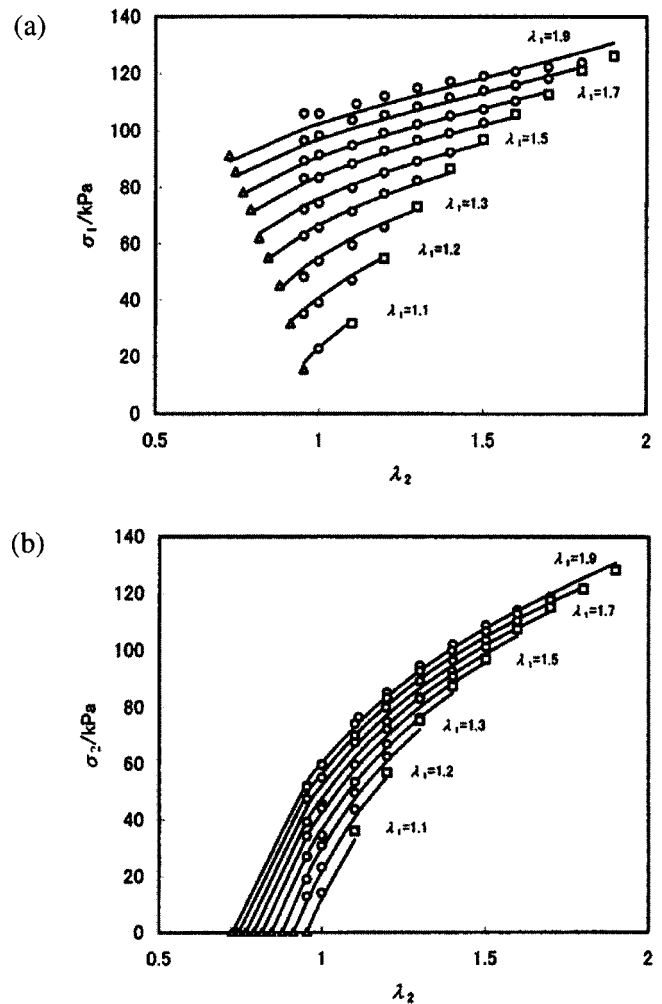


FIG. 2. Comparison of the theory with the quasi-equilibrium biaxial stress–elongation data (Ref. 21) of the end-linked PDMS network of $\phi_0=0.625$. λ_1 and λ_2 are the larger and smaller principal ratios in biaxial stretching, respectively, and σ_1 (a) and σ_2 (b) are the nominal stresses in the corresponding directions. The triangular and rectangular symbols stand for the data for the uniaxial ($\lambda_2=\lambda_1^{-1/2}$ and $\sigma_2=0$) and equibiaxial stretching ($\lambda_1=\lambda_2$), respectively. The solid lines represent the theoretical stress σ_i ($i=1,2$) at identical λ_1 as a function of λ_2 . The best-fitted parameters are $N_s/N_c=7.68$, $\eta=0.120$, $\alpha=0.160$, $h=0$.

condition: When the difference between the theoretical and experimental values of G_0 exceeds 10%, the corresponding value of N_s is discarded before fitting to the stress–strain data.

Figures 1–4 display the comparison of the biaxial stress–elongation data with the best-fit theoretical predictions for the end-linked PDMS networks prepared from melt, 70, 50, and 30 wt. %, respectively. The uniaxial data (shown by triangular symbols) are also included in the figures. The solid lines represent the theoretical stress as a function of λ_2 at constant λ_1 , where λ_1 and λ_2 are the larger and smaller principal ratios in biaxial stretching, respectively. The values of each parameter and Δ obtained in the best-fit procedure are listed in Table II. As can be seen in Figs. 1–4, the theoretical curves satisfactorily agree with the experimental data over the entire deformation range for all the samples. The stress–strain data involve the experimental error of $\pm 5\%$. The fitted curves lie within the error bars for most of the data

points, although the error bars are not shown in the figures in order to avoid overlapping. The good agreements are also confirmed by the small Δ values: The differences between the data and the theoretical predictions are less than 8%. The theoretical values of G_0 calculated from Eq. (6) with the best-fit parameters, shown in Table II are also in good accordance with the experimental values listed in Table I. Thus the predictions of the slip-link model successfully fit the biaxial data as well as G_0 for the end-linked PDMS networks with different entanglement densities. We discuss below how each of the best-fit parameters depends on network concentration.

The best-fit value of h was zero for all the networks. The condition $h=0$ corresponds to full suppression of thermal fluctuation of cross-link (affine limit). Patel *et al.*²⁷ reported $h=0$ for the melt-end-linked PDMS networks irrespective of entanglement density on the basis of the dependence of G_0 on ν , which accords with the result obtained here. According to the principle of end-linking, the molecular mass between

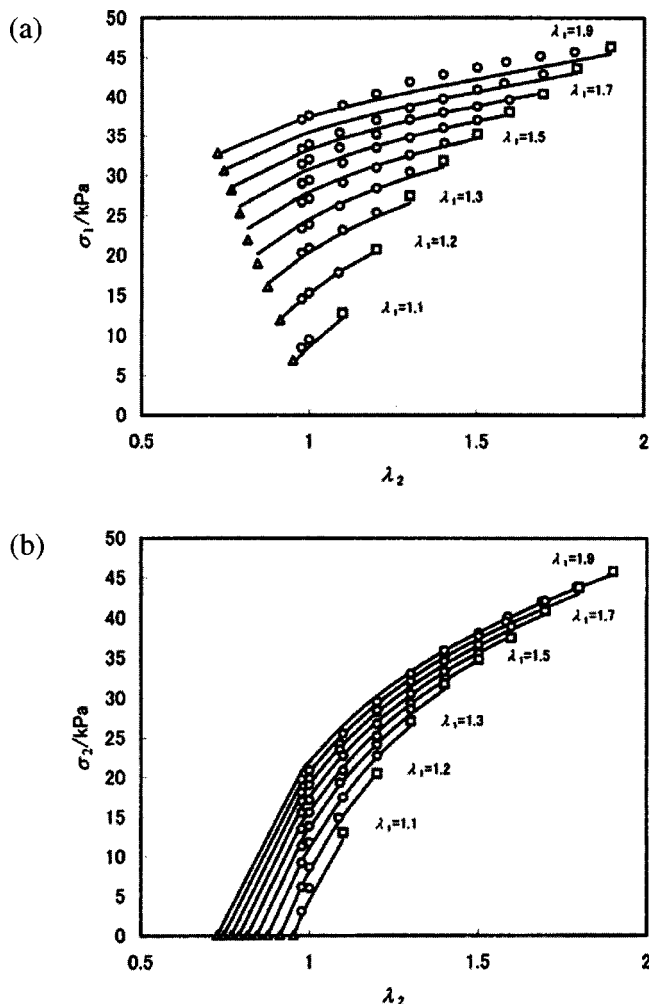


FIG. 3. Comparison of the theory with the quasiequilibrium biaxial stress-elongation data (Ref. 20) of the end-linked PDMS network of $\phi_0=0.463$. λ_1 and λ_2 are the larger and smaller principal ratios in biaxial stretching, respectively, and σ_1 (a) and σ_2 (b) are the nominal stresses in the corresponding directions. The triangular and rectangular symbols stand for the data for the uniaxial ($\lambda_2=\lambda_1^{-1/2}$ and $\sigma_2=0$) and equibiaxial stretching ($\lambda_1=\lambda_2$), respectively. The solid lines represent the theoretical stress σ_i ($i=1,2$) at an identical λ_1 as a function of λ_2 . The best-fitted parameters are $N_s/N_c=2.62$, $\eta=0.169$, $\alpha=0.134$, $h=0$.

adjacent cross-links is unaltered by dilution at preparation. Consequently, N_c is expected to vary linearly with ϕ_0 , when the degree of thermal fluctuation of cross-links (h) is not altered by dilution. In Fig. 5, the best-fit values of N_c appear to depend linearly on ϕ_0 , which agrees with the expectation.

Figure 5 also shows the double logarithmic plots of N_s vs ϕ_0 . The least square method yields $N_s \sim \phi_0^{2.4}$. Entanglement coupling (slip-link) originates from the binary interaction, which suggests that the ϕ_0 dependence of N_s obeys a power law with an exponent of two²⁸ or about 2.3.²⁹ The experimental exponent is slightly larger but close to the expected values. The ratio N_s/N_c represents the elastic contribution of entanglements relative to that of cross-links. As can be seen in Table II, N_s/N_c decreases with decreasing in ϕ_0 as a result of the reduction in entanglement density. The large values of N_s/N_c for the networks of $\phi_0 \geq 0.625$ indicate that the networks are entanglement-dominated. Actually, the magnitude of G_0 of the melt-end-linked network is reason-

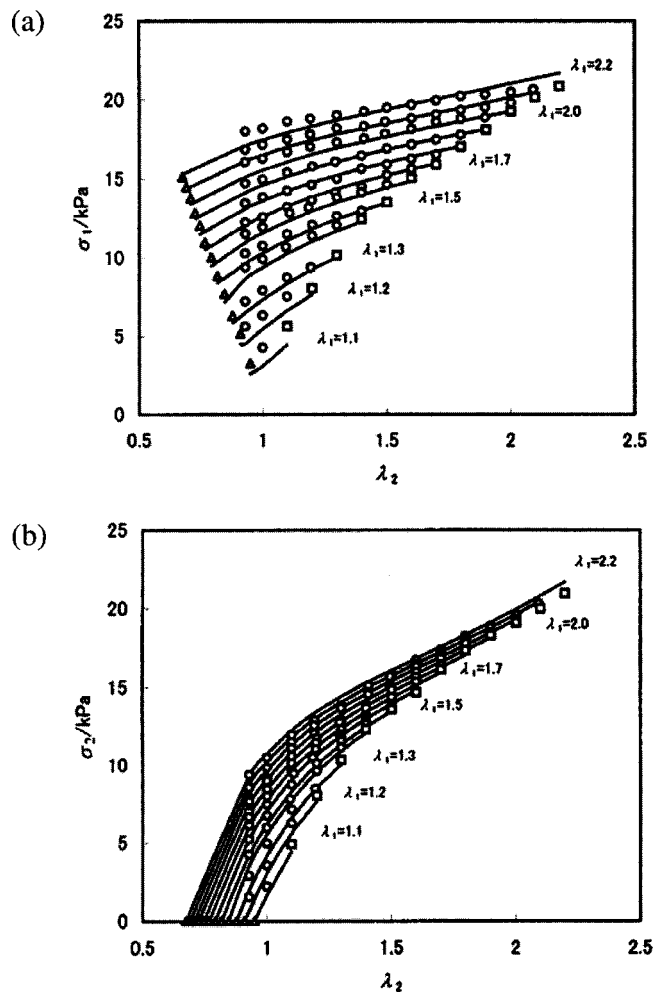


FIG. 4. Comparison of the theory with the quasiequilibrium biaxial stress-elongation data (Ref. 20) of the end-linked PDMS network of $\phi_0=0.283$. λ_1 and λ_2 are the larger and smaller principal ratios in biaxial stretching, respectively, and σ_1 (a) and σ_2 (b) are the nominal stresses in the corresponding directions. The triangular and rectangular symbols stand for the data for the uniaxial ($\lambda_2=\lambda_1^{-1/2}$ and $\sigma_2=0$) and equibiaxial stretching ($\lambda_1=\lambda_2$), respectively. The solid lines represent the theoretical stress σ_i ($i=1,2$) at identical λ_1 as a function of λ_2 . The best-fitted parameters are $N_s/N_c=1.57$, $\eta=0.799$, $\alpha=0.125$, $h=0$.

ably explained by the quasiplateau modulus of uncrosslinked entangled PDMS melt $G_N^0 (=2.0 \times 10^5 \text{ Pa})$ (Ref. 30) together with the consideration that the unreacted reactants act as diluent in network preparation, $G_N^0(0.92)^2 \sim 1.6 \times 10^5 \text{ Pa}$.

Figure 6 illustrates the best-fit values of η as a function of ϕ_0 . As ϕ_0 decreases, i.e., entanglement density decreases, η becomes larger. This tendency accords with the intuitive expectation from the physical meaning of η : η is a measure of slippage for slip-link. An increase in the distance between neighboring entanglements increases the freedom of the motion of slip-link. The quantitative relation of η with network structure is unknown at present, but Vilgis *et al.*³¹ proposed the following rough estimate:

$$\eta \approx M_e/M_c, \quad (8)$$

where M_e and M_c are the molecular weights between neighboring entanglements and cross-links, respectively. We em-

TABLE II. Best-fit parameter values and estimated values from molecular approaches.

ϕ_0	Δ^a /%	h	N_c /mol m ⁻³	N_s /mol m ⁻³	N_s/N_c	η	η_{est}^b	η_{est}^c	α	α_{est}^d	$G_{0,\text{cal}}^e$ kPa
0.914	7.84	0	5.88	52.8	8.98	0.105	0.111	0.141	0.178	0.199	147
0.625 ^f	3.58	0	3.22	24.7	7.68	0.120	0.130	0.194	0.160	0.161	67.0
0.463	4.10	0	3.02	7.91	2.62	0.169	0.382	0.293	0.134	0.116	24.9
0.283	6.75	0	2.12	3.33	1.57	0.799	0.637	0.510	0.125	0.0880	8.96

^aDefined by Eq. (7).^bEstimated from Eq. (9).^cEstimated from Eq. (10).^dEstimated from Eq. (11).^eCalculated from Eq. (6) with the best-fit parameter values.^fThe values of the best-fit parameters for the sample are slightly different from those published previously (Ref. 11) due to the difference in the best-fit procedures (Ref. 26).

ploy the following two methods for the estimation of M_e/M_c . As is evident from the definitions, M_e/M_c is equivalent to N_c/N_s ,

$$\eta \approx M_e/M_c = N_c/N_s. \quad (9)$$

Table II tabulates the η values calculated from Eq. (9) with the best-fit values of N_c and N_s . In the other approach, M_e/M_c was evaluated using $M_e = M_{e,\text{melt}}\phi_0^{-1}$ (Ref. 28) and $M_c = M_{n,\text{el}}$ as

$$\eta \approx M_e/M_c = M_{e,\text{melt}}\phi_0^{-1}/M_{n,\text{el}}. \quad (10)$$

The η values calculated by Eq. (10) and $M_{e,\text{melt}} = 10\,000$ g/mol for PDMS (Ref. 30) are listed in Table II. The values estimated from Eqs. (9) and (10) are slightly different but comparable. The agreement in η between the best-fit values and the estimates from Eq. (9) or (10) is more or less tolerable in view of the accessible range of η ($0 < \eta < \infty$) as well as the roughness included in the estimation.

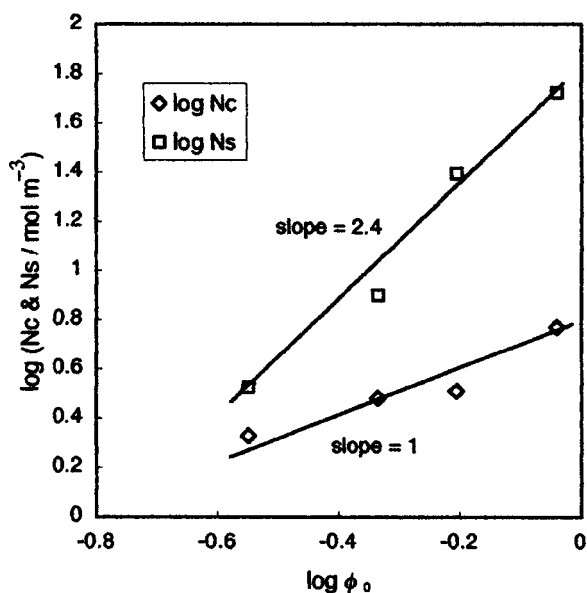
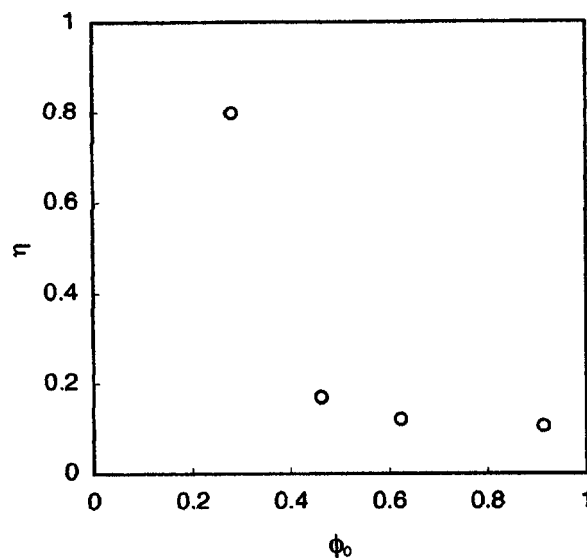
The ϕ_0 dependence of the best-fit values of α is shown in Fig. 7. The α values decrease with decreasing in ϕ_0 , i.e., entanglement density. This trend is physically reasonable because α is a measure of inextensibility ($\alpha = 1/\lambda_{\text{max}}$): A de-

crease in the number of entanglements increases the length of the network strand between neighboring entanglements, which increases the extensibility of network. The primitive path concept⁷ derives $\lambda_{\text{max}} = N_j^{1/2}$, where N_j is the number of the Kuhn segments between topologically adjacent cross-links or entanglements where cross-link and entanglement are not distinguished. The expression for α is obtained by using the relation between N_j and G_0 ,³²

$$\alpha \approx \left(\frac{1}{N_j}\right)^{1/2} = \left(\frac{G_0 m p}{c R T}\right)^{1/2}, \quad (11)$$

where m is the molecular mass of a repeating unit, p is the number of the repeating unit per one Kuhn segment, and c is the network concentration. For PDMS, $m = 74$ g/unit and $p = 8.5$.³³ The values of α calculated from Eq. (11), shown in Table I, are fairly close to the best-fit values. The accordance between the best-fit values and the estimates from Eq. (11) is considered satisfactory in view of the accessible range of α ($0 < \alpha < \infty$).

Thus the slip-link model satisfactorily describes the bi-axial stress-strain data of the end-linked PDMS networks with different entanglement densities. Each of the best-fit model-specific parameters (N_c, N_s, η, α) depends on net-

FIG. 5. The best-fitted values of N_c and N_s as a function of ϕ_0 .FIG. 6. The best-fitted values of η as a function of ϕ_0 .

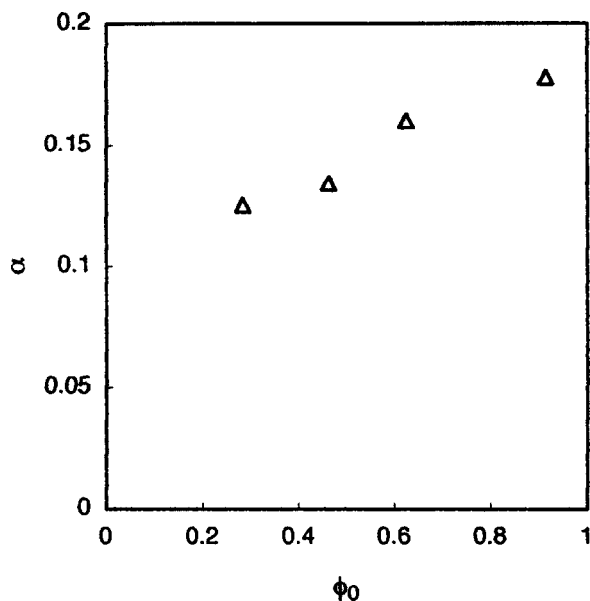


FIG. 7. The best-fitted values of α as a function of ϕ_0 .

work concentration (or entanglement density) in a physically reasonable way. In particular, the magnitudes of the best-fit values of η and α satisfactorily agree with the estimates from another molecular approaches independent of mechanical testing. These results suggest that the slip-link model successfully accounts for the chain-entanglement effects on rubber elasticity.

ACKNOWLEDGMENT

This work was partly supported by a Grant-in-Aid from the Ministry of Education, Science, Sports, and Culture of Japan (No. 13750831).

¹W. Kuhn, *J. Polym. Sci.* **1**, 380 (1946).

²L. R. G. Treloar, *Trans. Faraday Soc.* **42**, 77 (1946).

³H. M. James and E. Guth, *J. Chem. Phys.* **15**, 669 (1947).

⁴F. T. Wall and P. J. Flory, *J. Chem. Phys.* **19**, 1435 (1951).

⁵L. R. G. Treloar, *The Physics of Rubber Elasticity*, 3rd ed. (Clarendon, Oxford, 1975).

⁶A. Kloczkowski, J. E. Mark, and B. Erman, *Macromolecules* **28**, 5089 (1995).

⁷S. F. Edwards and T. A. Vilgis, *Polymer* **27**, 483 (1986); *Rep. Prog. Phys.* **51**, 243 (1988).

⁸R. J. Gaylord and J. F. Douglas, *Polym. Bull. (Berlin)* **18**, 347 (1987); **23**, 529 (1990).

⁹M. Kaliske and G. Heinrich, *Rubber Chem. Technol.* **72**, 602 (1999).

¹⁰M. Rubinstein and S. Panyukov, *Macromolecules* **30**, 8036 (1997).

¹¹K. Urayama, T. Kawamura, and S. Kohjiya, *Macromolecules* **34**, 8261 (2001).

¹²N. W. Tschoegl and C. Gurer, *Macromolecules* **18**, 680 (1985).

¹³M. G. Brereton and K. G. Klein, *Polymer* **29**, 970 (1988).

¹⁴S. Candau, A. Peters, and J. Herz, *Polymer* **22**, 1504 (1981).

¹⁵V. G. Vasiliev, L. Z. Rogovina, and G. L. Slonimsky, *Polymer* **26**, 1667 (1985).

¹⁶K. Urayama and S. Kohjiya, *J. Chem. Phys.* **104**, 3352 (1996); *Eur. Phys. J. B* **2**, 75 (1998).

¹⁷K. Urayama, T. Kawamura, and S. Kohjiya, *J. Chem. Phys.* **105**, 4833 (1996).

¹⁸K. Sivasailam and C. Cohen, *J. Rheol.* **44**, 897 (2000).

¹⁹D. R. Miller and C. W. Macosko, *Macromolecules* **9**, 206 (1976).

²⁰T. Kawamura, K. Urayama, and S. Kohjiya, *J. Polym. Sci., Part B: Polym. Phys.* **40**, 2780 (2002).

²¹T. Kawamura, K. Urayama, and S. Kohjiya, *Macromolecules* **34**, 8252 (2001).

²²R. C. Ball, M. Doi, S. F. Edwards, and M. Warner, *Polymer* **22**, 1010 (1981).

²³L. M. Dossin and W. W. Graessley, *Macromolecules* **12**, 123 (1979).

²⁴N. R. Langlely and K. E. Polmanteer, *J. Polym. Sci., Polym. Phys. Ed.* **12**, 1023 (1974).

²⁵D. J. Orrah, J. A. Semlyen, and S. B. Ross-Murphy, *Polymer* **29**, 1452 (1988).

²⁶In the previous paper (Ref. 11) the root of mean square (rms) $(1/2n) \times \{\sum_i \sum_n (\sigma_{i,th} - \sigma_{i,exp})^2\}^{1/2}$ was minimized for data-fitting. Due to the difference in the rms and Δ defined by Eq. (7), the best-fit parameter values for the network of $\phi_0=0.625$ are slightly different from those reported previously (Ref. 11). The rms tends to weight σ_1 relative to σ_2 due to the fact of $\sigma_1 \geq \sigma_2$ under any biaxial strains. This tendency is eliminated in Δ where the difference $|\sigma_{i,th} - \sigma_{i,exp}|$ is reduced by the stress $\sigma_{i,exp}$ ($i = 1, 2$).

²⁷S. K. Patel, C. Malone, C. Cohen, J. R. Gillmor, and R. H. Colby, *Macromolecules* **25**, 5241 (1992).

²⁸J. D. Ferry, *Viscoelastic Properties of Polymers* (Wiley, London, 1980).

²⁹P.-G. de Gennes, *Scaling Concepts of Polymer Physics* (Cornell University Press, Ithaca, 1979).

³⁰D. J. Plazek, W. Dannhuser, and J. D. Ferry, *J. Colloid Sci.* **16**, 101 (1961).

³¹T. A. Vilgis and B. Erman, *Macromolecules* **26**, 6657 (1993).

³²M. Doi and S. F. Edwards, *The Theory of Polymer Dynamics* (Oxford University Press, New York, 1986).

³³R. F. T. Stepto, in *Siloxane Polymers*, edited by S. J. Clarson and J. A. Semlyen (PTR Prentice-Hall, New Jersey, 1993).